JOURNAL OF GEOPHYSICAL RESEARCH, VOL. 99, NO. A11, PAGES 21,213–21,224, NOVEMBER 1, 1994

The source of Jovian auroral hiss observed by Voyager 1

D. D. Morgan, D. A. Gurnett, and W. S. Kurth
Department of Physics and Astronomy, University of Iowa, Iowa City

F. Bagenal
Department of Astrophysical, Planetary, and Atmospheric Sciences, University of Colorado, Boulder

Abstract. Observations of auroral hiss obtained from the Voyager 1 encounter with Jupiter have been reanalyzed. The Jovian auroral hiss was observed near the inner boundary of the warm Io torus and has a low-frequency cutoff caused by propagation near the resonance cone. A simple ray tracing procedure using an offset tilted dipole of the Jovian magnetic field is used to determine possible source locations. The results obtained are consistent with two sources located symmetrically with respect to the centrifugal equator along an L shell ($L \simeq 5.59$) that is coincident with the boundary between the hot and cold regions of the Io torus and is located just inward of the ribbon feature observed from Earth. The distance of the sources from the centrifugal equator is approximately $0.58 \pm 0.01\ R_J$. Based on the similarity to terrestrial auroral hiss, the Jovian auroral hiss is believed to be generated by beams of low energy (~tens to thousands of eV) electrons. The low-frequency cutoff of the auroral hiss suggests that the electrons are accelerated near the inferred source region, possibly by parallel electric fields similar to those existing in the terrestrial auroral regions. A field-aligned current is inferred to exist at L shells just inward of the plasma ribbon. A possible mechanism for driving this current is discussed.

1. Introduction

Auroral hiss is a type of whistler mode radiation commonly observed over the Earth's auroral zone. Auroral hiss is characterized by a funnel-shaped, low-frequency cutoff with the central axis of the funnel coinciding with regions of intense auroral precipitation. An example of auroral hiss detected by the Dynamics Explorer 1 spacecraft is shown in Figure 1. This type of VLF noise is observed on virtually every auroral zone pass at radial distances between 2 and 4 R_E [*Gurnett et al.*, 1983]. *Smith* [1969], *Mosier and Gurnett* [1969], *James* [1976], and others have explained the funnel-shaped, low-frequency cutoff as a propagation effect caused by wave vectors near the whistler mode resonance cone.

The formation of the funnel-shaped spectrum can be understood as follows. Auroral hiss is known to propagate at wave normal angles very close to the resonance cone. The condition for a resonance cone angle θ_{Res} is found by allowing the index of refraction to go to infinity in the cold plasma dispersion relation. The resonance cone angle is given by

$$\tan^2 \theta_{\text{Res}} = -P/S$$

where the functions P and S are defined by *Stix* [1962]. For propagation near the resonance cone the ray path is nearly perpendicular to the wave normal vector. The angle ψ of the ray path relative to the magnetic field is given approximately by

$$\cot^2 \psi = -P/S.$$

Paper number 94JA01904.
0148-0227/94/94JA-01904$05.00

The regime of interest has $|f_{ce}| \ll f_{pe}$ and $|f_{ci}| \ll f \ll |f_{ce}|$ so that $P \approx -(f_{pe}/f)^2$ and $S \approx (f_{pe}/f_{ce})^2\ [1 - (f_{LHR}^2/f^2)]$. Here f is the wave frequency, f_{ce} the electron cyclotron frequency, f_{pe} the electron plasma frequency, f_{ci} the ion cyclotron frequency, and f_{LHR} the lower hybrid frequency, given by $|f_{ce}f_{ci}|^{1/2}$ when only one species of ion dominates [*Gurnett et al.*, 1979]. From these approximations it can be shown that the ray angle ψ is then given by

$$\tan^2 \psi = \frac{f^2 - f_{LHR}^2}{f_{ce}^2} \tag{1}$$

Equation (1) implies that the ray path angle increases with increasing frequency. Figure 2 schematically shows how (1) leads to the filled-in funnel shape typically detected for auroral hiss. (The numbers used here are meant only to be illustrative and do not correspond to actual measurements.) When the spacecraft is at position 1, it detects noise generated by the electron beam. Of the three source points A, B, and C, the ray angle for radiation reaching the spacecraft is smallest from point A. From (1) it can be seen that radiation that originates from point A must have the lowest frequency of radiation detected by the spacecraft. At spacecraft position 2 the radiation generated at source point A still has the lowest frequency. However, all frequencies are now lower because all ray angles are smaller. Thus as the spacecraft approaches the source field line, the frequency of radiation detected from each source point decreases. Note that because point A is the farthest of the source points from the spacecraft, it is always emitting rays at the smallest ray path angle and therefore defines the low-frequency limit of the hiss emitted from the source beam. The existence of the low-frequency cutoff implies that there is a lower limit to the source region, represented in the diagram by point A. All

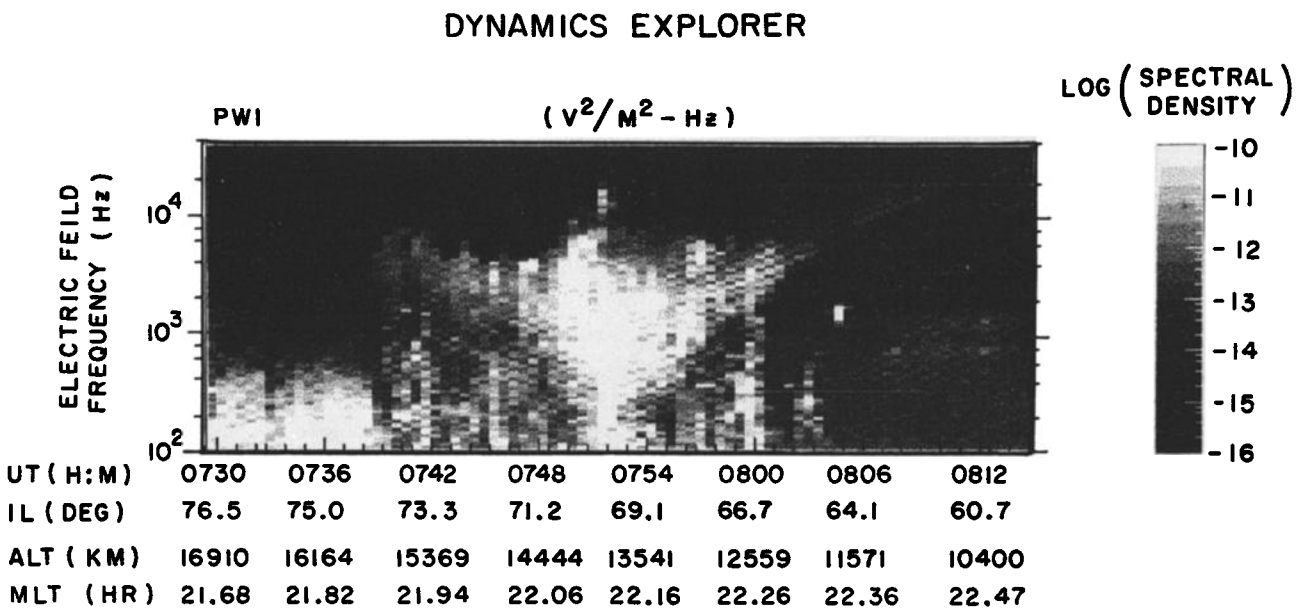

Figure 1. An example of terrestrial auroral hiss, observed by the Dynamics Explorer 1 spacecraft, displaying the funnel-shaped cutoff. The figure shows a wave electric field spectrogram of an auroral hiss event on August 26, 1981. The horizontal axis indicates universal time (UT), invariant latitude (IL), altitude (ALT) in kilometers, and magnetic local time (MLT); the vertical axis indicates frequency; and the shade of gray indicates electric wave spectral density.

points between point A and the path of the spacecraft emit rays at a larger angle relative to the magnetic field than does point A and therefore have higher frequencies. These rays fill in the funnel in the spectrogram. Evidence that the wave vector of auroral hiss is close to the resonance cone is given by *Smith* [1969], *Mosier and Gurnett* [1969], *James* [1976], and *Gurnett et al.* [1983]. This last reference gives a more general version of (1) and a more detailed version of this argument.

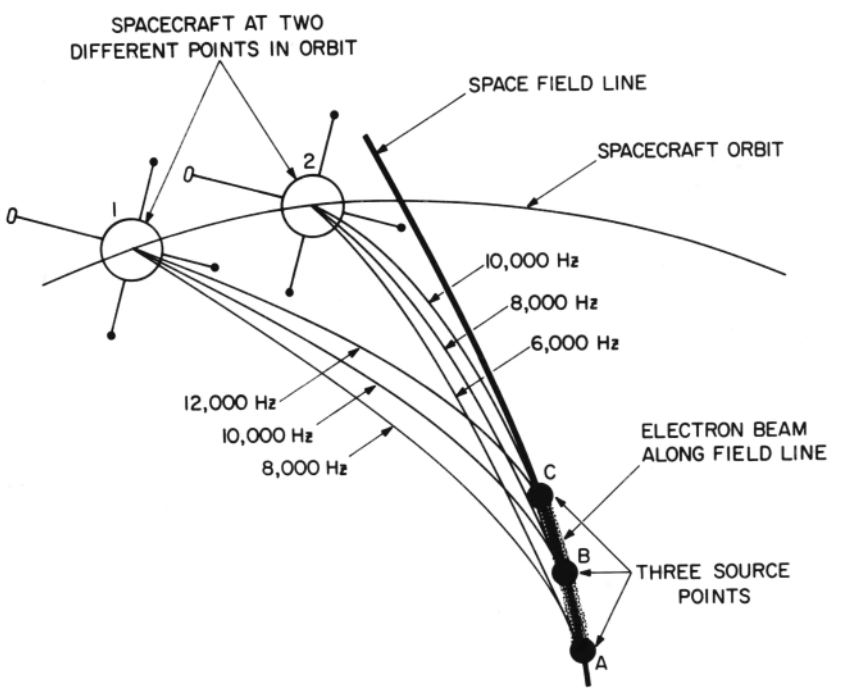

Figure 2. Schematic explanation of the funnel-shaped, low-frequency cutoff observed in auroral hiss spectrograms. As the spacecraft approaches the source field line, auroral hiss is detected at decreasing frequencies. As is shown in the diagram the lowest frequency detected at a given spacecraft position will be determined by the emission originating at the source point farthest from the spacecraft position, in accordance with (1). Thus if a minimum frequency is detected, a spatial limit to the source region can be inferred. The frequencies cited are merely illustrative and not the result of calculation.

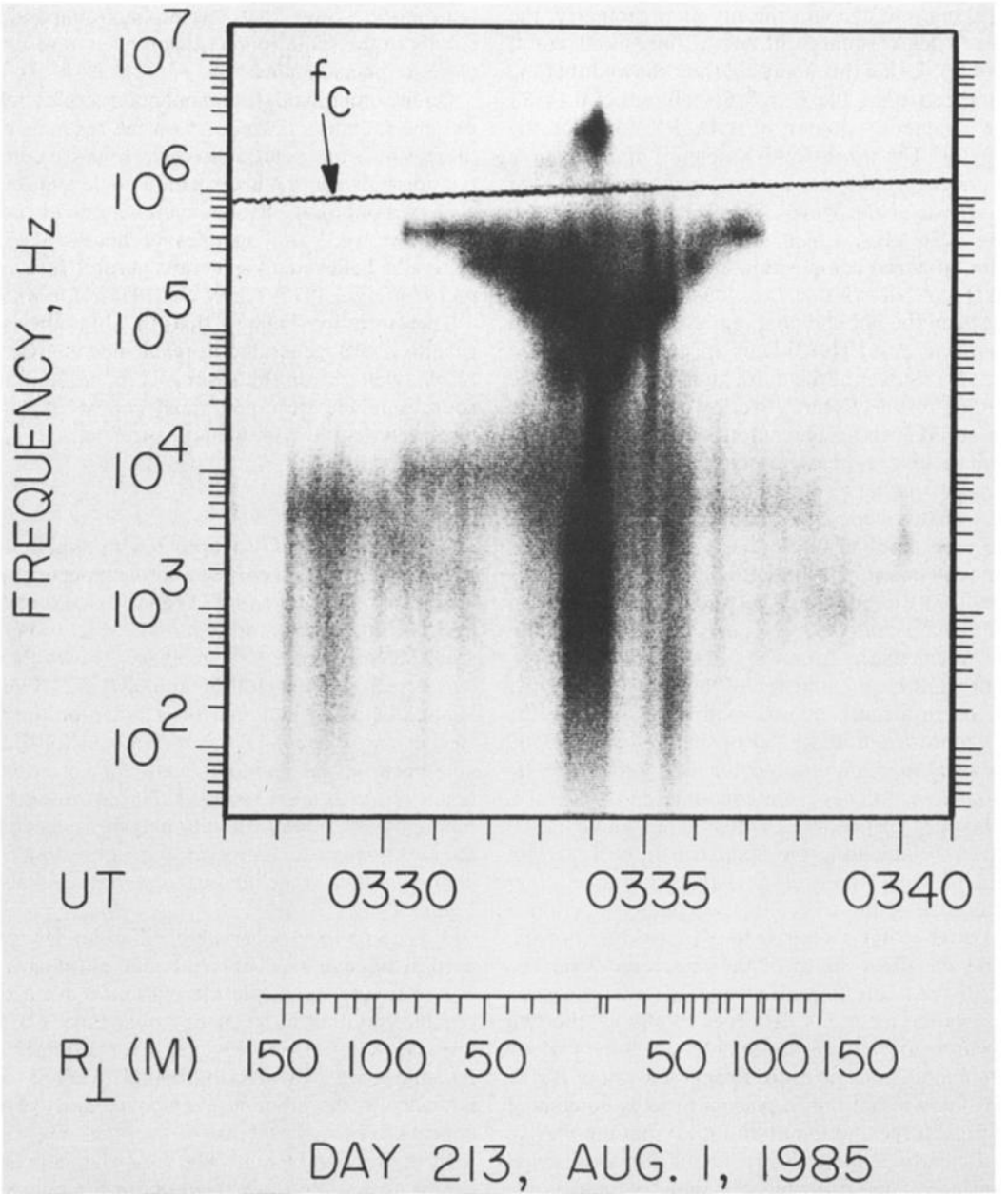

Figure 3. A time-frequency-intensity spectrogram showing whistler mode noise generated by an electron gun aboard Spacelab 2. Note the well-defined funnel shape and the upper cutoff near the electron cyclotron frequency. The base of the funnel coincides with the Plasma Diagnostics Package (PDP) detector crossing the field line along which the source electron beam was launched. (From *Gurnett et al.* [1986].)

A number of studies associate electron beams with the generation of auroral hiss. *Gurnett* [1966] showed that auroral hiss is associated with intense fluxes of precipitating low-energy (~10 keV) auroral electrons near the poleward edge of the 40-keV trapping boundary. *Gurnett and Frank* [1972] observationally associate auroral hiss with intense electron beams of energies on the order of hundreds of eV. *Lin et al.* [1984] conducted a study of five cases of dayside auroral hiss in which the hiss was associated with electron beams of energies up to 100 eV. Further evidence of an electron beam source for auroral hiss was demonstrated by an active experiment aboard Spacelab 2, reported by *Gurnett et al.* [1986]. On the Spacelab 2 mission a spacecraft known as the Plasma Diagnostics Package (PDP) was flown across the magnetic field line along which a 1-keV electron beam was being injected by an electron gun aboard the space shuttle. Figure 3, from *Gurnett et al.* [1986], shows a spectrogram of the wave electric field detected by the PDP. The funnel-shaped spectrum can be explained if it is assumed that the noise was created by the Landau resonance, that is, $v_{beam} = \omega/k_\parallel$. Ray tracing indicated that the funnel shape is consistent with whistler waves propagating near the resonance cone. Further analysis of this experiment by *Farrell et al.* [1988, 1989] showed that incoherent Cerenkov radiation could not generate the observed intensities but that a coherent bunching instability could.

The auroral hiss observed by Voyager 1 near Jupiter was first analyzed by *Gurnett et al.* [1979] shortly after the

encounter. Taking into account the ray path geometry, the authors made a least squares fit of the measured cutoff frequencies to (1). Using this analysis, they showed that the source was located along the $L = 5.6$ shell, either 0.14 R_J south of the magnetic equator or 1.16 R_J north of the magnetic equator. The north-south ambiguity in the source position arises because the instrument cannot determine the direction of arrival of the wave. The best fit analysis also gave $f_{LHR} = 1.56$ kHz, which is somewhat higher than expected from on-board composition analysis. *Bagenal and Sullivan* [1981] have shown that $L \cong 5.6$ corresponds to the boundary between the hot and cold regions of the Io plasma torus. *Gurnett and Scarf* [1983] later speculated that there were actually two sources at the north and south edges of the torus. According to this picture, two low-frequency cutoffs should be observed. This second cutoff, which has now been identified, will be discussed later.

Auroral hiss emanating from the Io plasma torus is not the only form of whistler mode emission observed near Jupiter. The recent Ulysses flyby of Jupiter has yielded observations of whistler mode emissions apparently emitted at high magnetic latitude from the boundary between open and closed field lines [*Farrell et al.*, 1993]. These emissions are not related to those emanating from the torus region.

The present work is an extension of the study by *Gurnett et al.* [1979] using a more refined method of locating the source and a more accurate model of the Jovian magnetic field. We have refined the source location procedure by actually tracing the cutoff ray paths encountered at several L values. In this tracing procedure an offset tilted dipole (OTD) model was used, eliminating the approximation of straight magnetic field lines used in the original analysis of *Gurnett et al.* [1979]. Because of the directional ambiguity mentioned above, each cutoff profile gives rise to two possible sources, one north and the other south of the spacecraft location. Because two distinct cutoffs were visible, the analysis gives four possible source locations. In order to choose the two most likely sources from the four possible locations, various symmetry arguments must be used. From the work of *Hill et al.* [1974] it is known that the Io plasma torus is dominated by the centrifugal force due to corotation so that the plasma is distributed nearly symmetrically about the centrifugal symmetry surface. The centrifugal symmetry model has been used by *Bagenal and Sullivan* [1981] and *Bagenal et al.* [1985] to produce a contour map of the ion charge density in the Io plasma torus based on force balance between pressure gradient, centrifugal, ambipolar electric, and mirror forces. This density model will be used in our analysis.

It is possible that the existence of two low-frequency cutoffs could be attributed to a single source radiating at two solutions of the resonance condition, similar to the conversion mechanism described by *Bell and Ngo* [1990]. K. Maeda and W. Calvert (personal communication, 1994) claim to have seen such "saucers within saucers." Examination of the relation between propagation angle and frequency shows that for the present case, dual saucers are possible only near the minimum in $n_{\|}$, equivalent to the maximum in resonance energy. In the present case the maximum resonance energy is about 1650 eV, and dual saucers are possible only down to about 1300 eV. At lower values of the resonance energy, the monotonic relation between propagation angle and frequency deteriorates rapidly. Furthermore, analysis of the relation between the propagation angle and the frequency for both modes shows that it is probably impossible to fit both cutoffs to the same source region even at resonance energies close to the maximum.

On the other hand, for resonance energies below about 300 eV, the radiation is well out on the resonance cone, where there is only one solution to the resonance condition and the relation between the propagation angle and the frequency is always monotonic. Resonance energies in the hundreds of eV agree well with energies of beams at Earth that are generally believed to generate auroral hiss [see *Laaspere and Hoffman*, 1976; *Lin et al.*, 1984; *Morgan et al.*, 1994].

Therefore we believe that the hypothesis that Jovian auroral hiss is generated at resonance energies of hundreds of eV, well out on the resonance cone, and at two distinct sources is the best and most robust explanation of the observed dual low-frequency cutoff.

2. Observations

The encounter of Voyager 1 with Jupiter took place on March 5, 1979, with closest approach occurring around 1204 spacecraft event time (SCET) at a Jovicentric distance of 4.9 R_J. The spectrogram in Figure 4, which was obtained from the 16-channel spectrum analyzer, shows that auroral hiss was detected between 0930 and 0941 SCET on the inbound leg and between 1310 and 1410 SCET on the outbound leg. Because no wideband data are available for the outbound leg and because the contour plots for interpretation of our results from *Bagenal et al.* [1985] are based solely on the inbound data, no ray-tracing analysis has been attempted for the outbound case. However, it is interesting to compare the characteristics of the inbound and outbound hiss as shown in Figure 4.

There are four observable differences between the two auroral hiss events. (1) The inbound event has a well-ordered rise in frequency, while the outbound event exhibits a less regular variation in frequency over time. (2) The outbound event is visible from Voyager 1 for a longer time than the inbound event. (3) The outbound event is comparable in intensity to the inbound event over most of its extent but appears to be more intense at the outer edge of detectability than the inbound event. The four channels for which both events are visible show the outbound event as more intense by an average factor of 1.5. The difference in intensity at the outer edge is more obvious from line plots than from the present figure. (4) The outbound event is observable at both higher and lower frequencies than the inbound event.

It is also instructive to look at spacecraft position while auroral hiss is being detected. Figure 5 shows the path of the spacecraft in cylindrical coordinates relative to the centrifugal equator. The shaded portions of the orbit indicate where the spacecraft was when the auroral hiss was detected. Figure 5 shows that the outbound event was observable over a larger region than the inbound event. Analysis of the L shells indicates that the outer edge of detection of both events was at $L = 5.6$. However, the inner edge of the inbound event was $L = 5.5$ while the inner edge of the outbound event was $L = 5.1$. Since the outer edge of the auroral hiss is probably near to the source L shell, this figure shows that the auroral hiss emitted from the outbound source reaches L shells farther from the source than that from the inbound source.

Figure 6 shows the same data projected on the equatorial

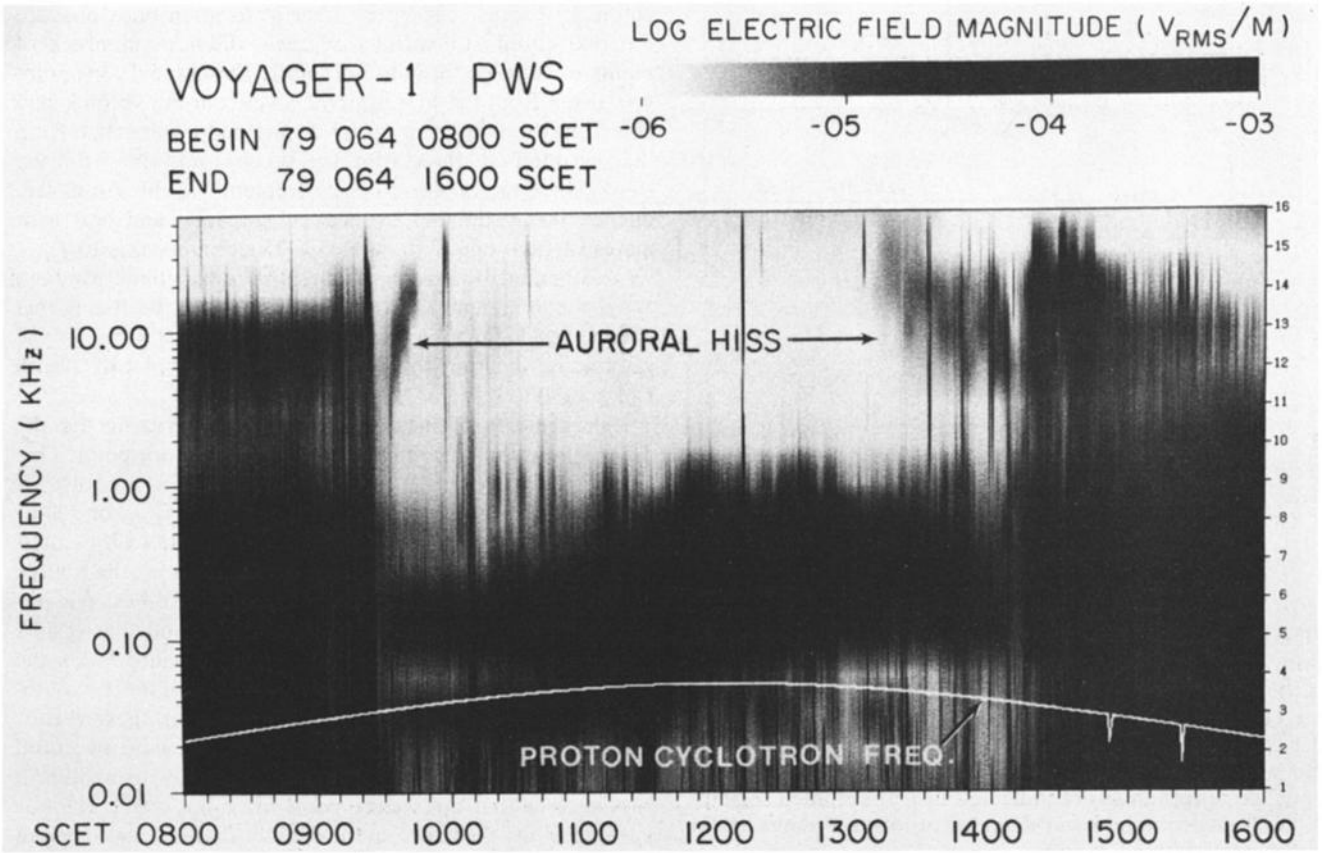

Figure 4. Time-frequency-wave electric field spectrogram displaying data for several hours around closest approach of Voyager 1 to Jupiter. The horizontal axis shows spacecraft event time (SCET) in hours, the vertical axis shows frequency in kilohertz, and the shade of gray indicates the rms electric field in volts per meter. Auroral hiss is visible between about 0930 and 0945 SCET (inbound) and 1310 and 1410 SCET (outbound). Note that the auroral hiss is more intense and of longer duration for the latter period. The proton cyclotron frequency contour is calculated from the Voyager magnetometer observations obtained via the Planetary Data System.

plane of Jupiter. Io's orbit is also shown. The shaded parts of the orbits indicate positions of both Voyager 1 and Io while auroral hiss was detected. Note the proximity of Io to the spacecraft during the detection of hiss on the outbound leg. Note also that Io travels along its orbit at 17 km/s, while the corotating plasma at this radius is moving at 74 km/s. Thus Voyager was just upstream of Io when hiss was detected on the outbound leg between 1310 and 1410 SCET.

We can draw the following conclusions based on the foregoing comparison of the inbound and outbound events. (1) Auroral hiss detected near Io is less well-ordered in frequency than that detected far from Io. (2) The outer edge of the region where hiss is detected is the same near to or far from Io, but close to Io, the auroral hiss is detected at much lower L shells. (3) The maximum intensity of auroral hiss detected near Io is greater than that detected far away from Io. (4) Auroral hiss generated near Io has a larger frequency range.

Figure 7 shows the three available segments of broadband data available during the time in which the auroral hiss was observed on the inbound leg of the orbit of Voyager 1. Low-frequency cutoffs for higher and lower frequency auroral hiss components are indicated by arrows. Note also minima in the spectra at 2.4 and 7.2 kHz. These minima are caused by notch filters in the instrument. They interfere with the cutoff frequency determination at certain times during the course of the emission. An analysis of the cutoff frequencies is described in the next section.

3. Analysis and Results

An analysis of the low-frequency cutoffs described in the previous section was done by using (1) in conjunction with an OTD model of the Jovian magnetic field. The OTD model chosen is based on the O4 model of *Acuña et al.* [1983]. The parameters used in this model are summarized in Table 1.

In order to calculate the angle of propagation relative to the magnetic field line, the cutoff frequency, the electron cyclotron frequency, and the lower hybrid frequency are needed. The cutoff frequency as a function of time was measured from spectrograms similar to Figure 7 but expanded in time. At each given time the Voyager 1 orbit data give the position of the spacecraft. The electron cyclotron frequency was determined using the OTD model for the Jovian magnetic field. The present method suffers a slight disadvantage compared to the method of *Gurnett et al.*

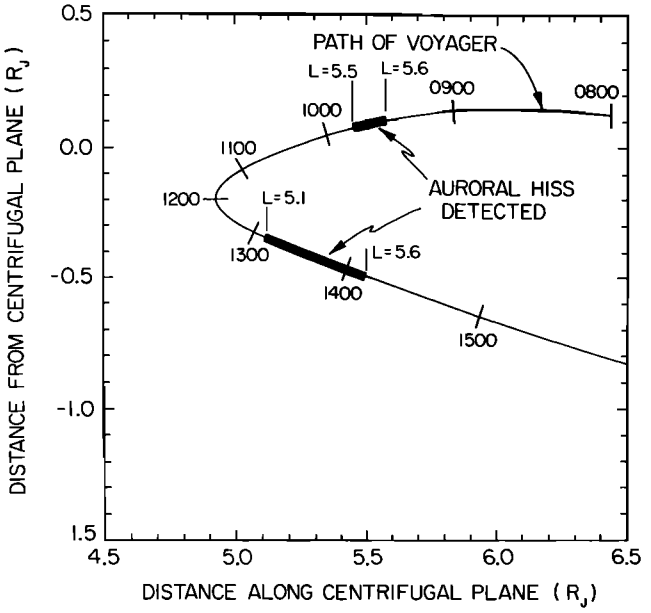

Figure 5. The path of Voyager 1 near closest approach in centrifugal-cylindrical coordinates (i.e., the horizontal axis is the distance from the position of the dipole projected on the centrifugal plane; the vertical axis is the distance from the centrifugal plane). Shaded parts of the orbit are where the auroral hiss is detected; L shells where Voyager 1 detected auroral hiss are indicated near the shaded regions. Note that auroral hiss was detected at lower L shells on the outbound orbit of Voyager 1.

[1979] in that there is no way of determining the lower hybrid frequency of the plasma. To test the sensitivity to variations in f_{LHR}, the calculations were performed using two values of f_{LHR}, both from *Gurnett et al.* [1979]. The value of f_{LHR} obtained by *Gurnett et al.* [1979] using a least squares fit procedure was 1.56 kHz. However, on the basis of the estimated composition of the Io plasma torus, they cite 300–500 Hz as a more likely value. The effects of varying f_{LHR} between 300 and 1560 Hz are included in the error bars shown in section 4.

The ray tracing is accomplished as follows. The electron cyclotron frequency at the spacecraft is calculated using the OTD magnetic field model from Table 1. Since f_{ce} and f_{LHR} have been estimated, the ray angle ψ can be calculated. The ray is traced at angle ψ from the magnetic field line in increments of 0.0001 R_J. After each step the electron cyclotron frequency is recalculated, giving a new value of ψ, and the procedure is repeated. Ray tracing is done both north and south from the spacecraft position because the Voyager plasma wave measurements do not indicate direction of propagation. Each of the two low-frequency cutoffs generates two possible ray paths. Possible sources are determined by the points where the ray paths converge at different frequencies.

Data points were taken from each of the three wideband data intervals illustrated in Figure 7. Spectrograms of the three intervals were enlarged and adjusted in intensity to give optimum resolution of the cutoff profiles. The lower of the two cutoff frequencies, previously analyzed by *Gurnett et al.* [1979], is referred to as cutoff 1, as labeled in Figure 7; the higher of the two cutoff frequencies is referred to as cutoff 2. Because the notch filter absorption lines obscure the two cutoffs to various degrees, different numbers of points were taken for cutoffs 1 and 2. For cutoff 1, one point was taken from the first interval, five from the second, and five from the third. For cutoff 2, one point was taken from the first interval, three from the second, and five from the third. Uncertainty due to measurements of the cutoff frequency was estimated by taking high, low, and best estimates of both cutoff frequencies. Uncertainty due to f_{LHR} was estimated by tracing each set of data points for both f_{LHR} = 300 Hz and f_{LHR} = 1560 Hz. Each ray tracing that is done results in a diagram similar to Figure 8, which is the ray-tracing diagram for the high estimate of cutoff 2 with f_{LHR} = 300 Hz.

Enlargements of these diagrams are used to locate the point where the traced rays best converge to a point. One cutoff frequency measurement was taken for a choice of direction from the spacecraft, cutoff 1 or 2, f_{LHR} of 300 or 1560 kHz, and upper, lower, or best estimate of the cutoff frequency. Thus a total of 24 measurements of the source position were made. In each case the point of best convergence was judged by eye and measured by hand. The results for all of these measurements are shown in Figure 9a, for the northern magnetic hemisphere, and Figure 9b, for the southern magnetic hemisphere. It can be seen from these results that the source point for the "best" estimate of the cutoff does not always fall between the high and low estimates. It is also clear that the source point for f_{LHR} = 300 Hz was systematically farther from the equator than the source point for f_{LHR} = 1560 Hz. However, the most important characteristic of Figures 9a and 9b is that the results for both sets of cutoffs form clusters of points that are clearly distinguishable from each other. Thus each cutoff yields two distinct source locations, one to the north and one to the south of the spacecraft.

However, each funnel-shaped cutoff is generated by only one source. Therefore some criterion is required for choosing one pair of possible sources over the other. According to

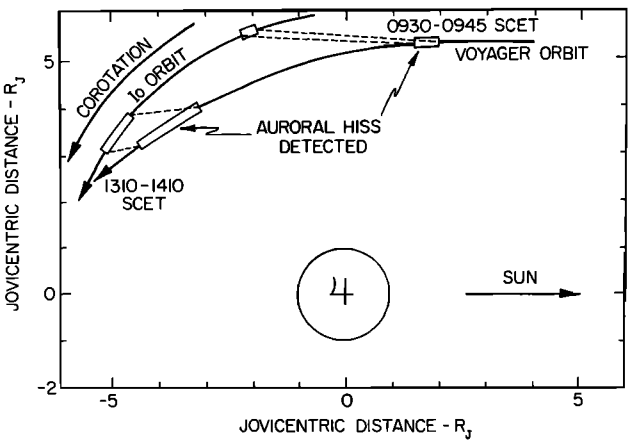

Figure 6. Orbits of Voyager 1 and Io projected on the equatorial plane of Jupiter. Boxed portions of both orbits indicate positions where auroral hiss is detected. The torus plasma overtakes Io at about 57 km/s so that Voyager 1 is actually upstream of Io during both periods of auroral hiss detection. From Figures 4 and 5 it is clear that the auroral hiss is more intense and extends to lower L shells when the spacecraft is closer to Io.

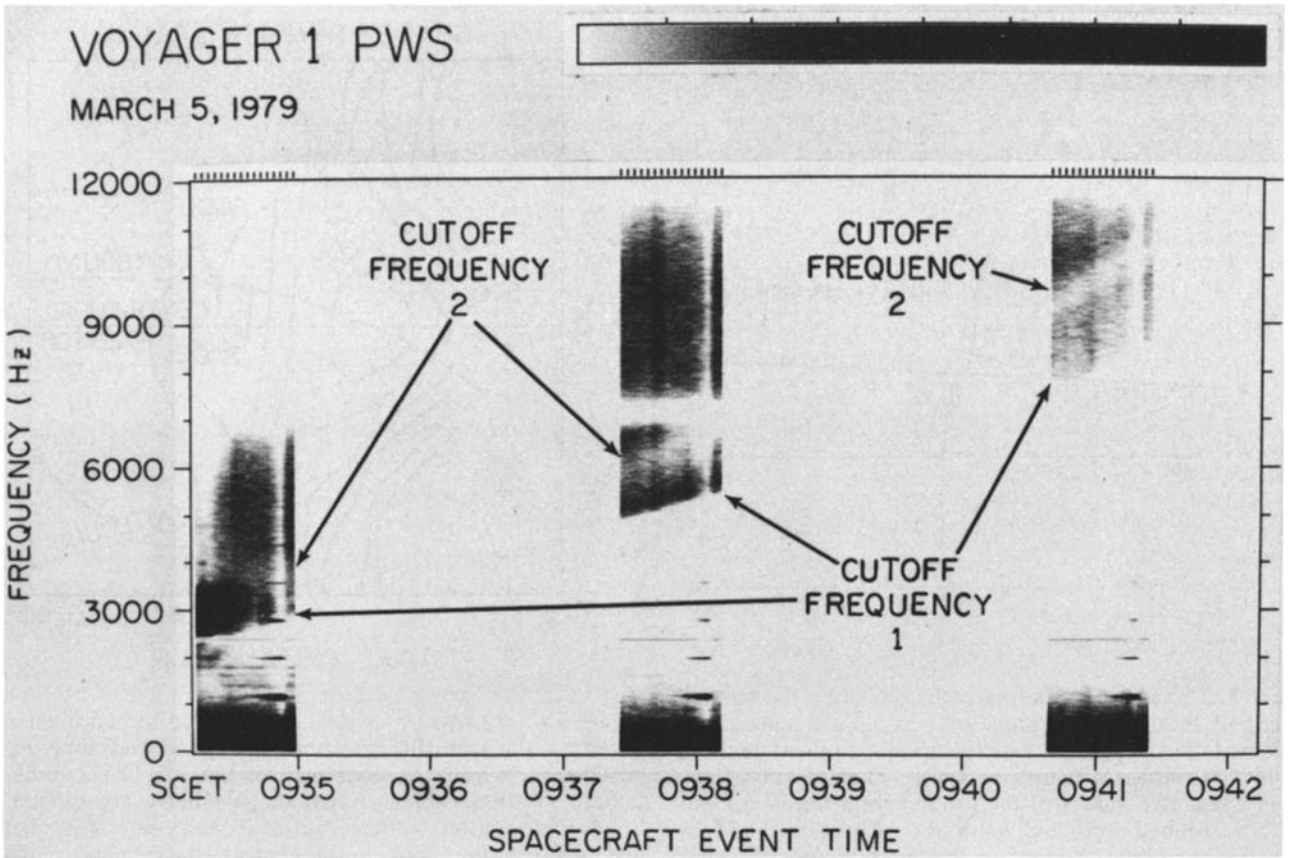

Figure 7. Mosaic of the wideband data showing the three data segments from which the two low-frequency cutoffs are measured. The two cutoffs are labeled 1 and 2, with cutoff 1 being the lower in frequency of the two. The horizontal axis indicates spacecraft event time, the vertical axis indicates frequency, and the shade of gray indicates strength of the wave electric field. Because the electric field detector utilized automatic gain control, the electric field measured is a relative rather than an absolute measurement. Intensity minima at 2.4 and 7.2 kHz are caused by notch filters within the instrument and should not be mistaken for auroral hiss cutoffs.

Hill et al. [1974], the structure of the Io plasma torus should be approximately symmetric about the centrifugal symmetry surface, with maximum plasma density occurring there. We have chosen to use maximum symmetry about the centrifugal symmetry surface as the criterion for choosing the correct set of sources. The possibilities exist that the sources could be asymmetric about the centrifugal symmetry surface, that they could be both on one side, or even that they could be generated by a single source. We believe that the essential symmetry of the physics of this region overwhelmingly favors the symmetric solution and that the single-source hypothesis is unlikely for reasons explained in section 1. The centrifugal symmetry surface is defined as the locus of points farthest from the spin axis of the planet on that point's magnetic field line and is closely approximated by a plane through the dipole at an angle β to the magnetic equator given by

$$\tan \beta = \tfrac{2}{3} \tan \alpha \qquad (2)$$

where α is the dipole tilt angle. This equation is a close approximation to equation (2) of *Hill et al.* [1974]. We shall refer to the plane defined by this equation as the centrifugal equator. The source locations have been plotted in a coordinate system based on this approximation to the centrifugal symmetry surface and superimposed on the ion density contour map from *Bagenal et al.* [1985]. The result is shown in Figure 10, wherein the possible source locations are shown as error bars. Maximum symmetry with respect to the centrifugal equator is achieved by assigning the source for cutoff 1 to the southern hemisphere and the source for cutoff 2 to the northern hemisphere. These source positions are identified by circles on the plot. The numerical results, given in Table 2, are found by taking the mean and error on the mean of the six points in each cluster shown in Figure 9. Results for the preferred source positions are the upper cutoff for the northern hemisphere and the lower cutoff for the southern hemisphere.

Table 1. Parameters Used in the Offset Tilted Dipole Model of the Jovian Magnetic Field

Parameter	Value
Tilt from rotation axis, deg	9.6
Longitudinal direction of tilt, deg	202 (System III)
Offset vector	
Length, R_J	0.131
Longitude, deg	148.6 (System III)
Latitude, deg	−8
Dipole strength, TR_J^3	4.28×10^{-4}

See *Acuña et al.* [1983].

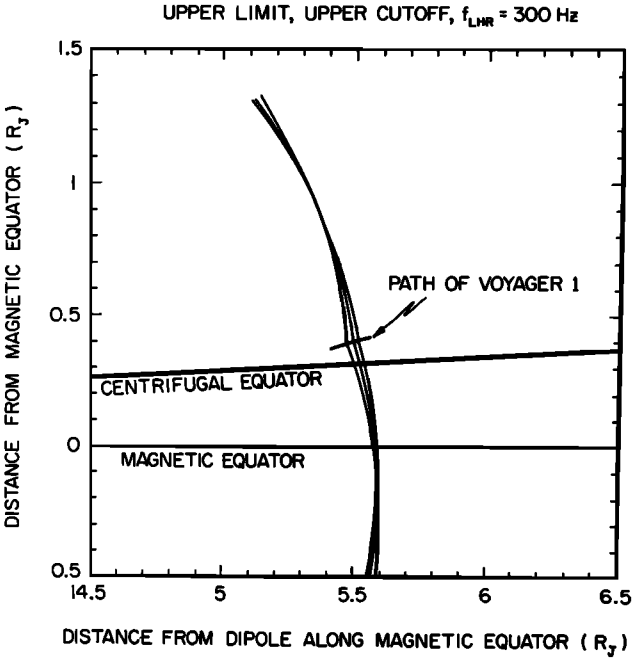

Figure 8. Example of the ray paths traced by the method described in the text. Points of best convergence were measured from ray trace diagrams similar to this figure but expanded in scale. Measurements were taken of cutoff 1 and cutoff 2, for two values of the lower hybrid frequency; for sources assumed north and south of the spacecraft; and for high, low, and best estimate of the cutoff frequency. Thus there were a total of 24 source position measurements.

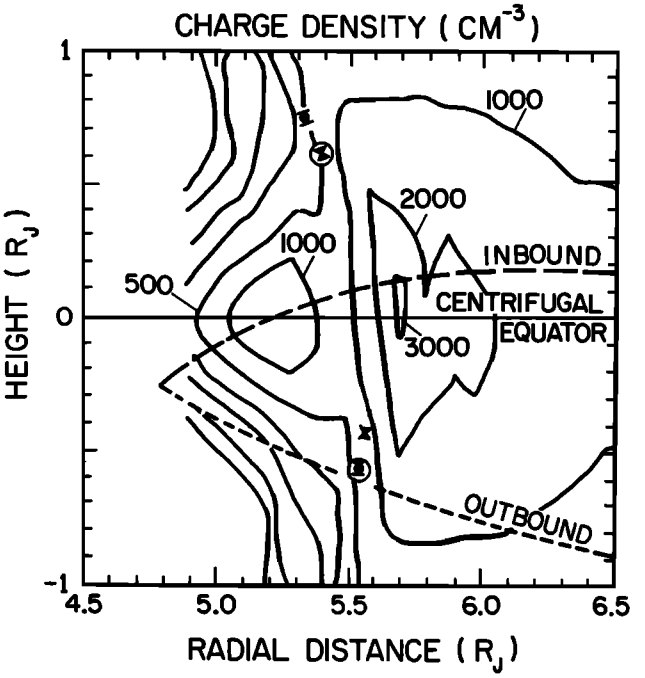

Figure 10. Results of analysis transformed to coordinates based on the centrifugal symmetry surface and superimposed on a density contour map of the Io plasma torus. Source location choices based on symmetry are circled. Solid circle, cutoff 1; cross, cutoff 2. Axes refer to radial distance from the dipole in the centrifugal symmetry plane and vertical distance from the centrifugal symmetry plane. (Adapted from *Bagenal et al.* [1985]).

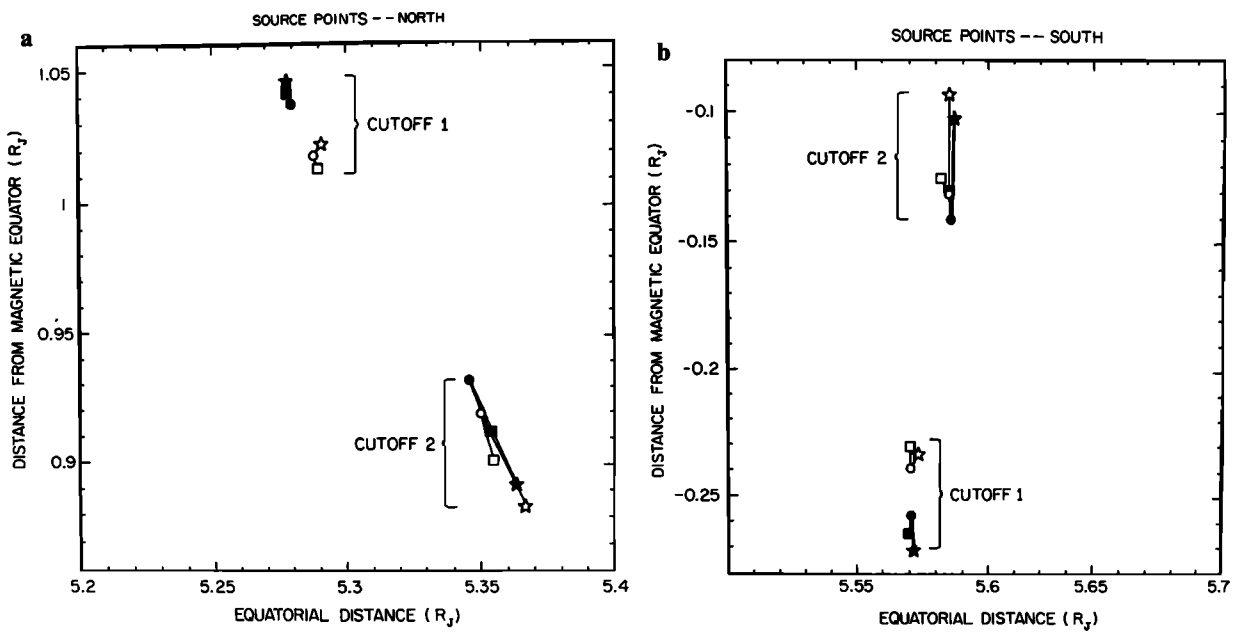

Figure 9. Summary of the 24 source position measurements. The measurements fall naturally into four clusters, each containing six points. The four clusters are identified as corresponding to possible sources north and south of the spacecraft derived from cutoffs 1 and 2. The points in each cluster measured for high, low, and best estimate of the cutoff frequency, with f_{LHR} = 300 Hz or 1560 Hz, are indicated by the legend. (a) Possible sources north of the centrifugal equator. (b) Possible sources south of the centrifugal equator. Correspondence between cutoffs 1 and 2 and the various source determinations is indicated in the figure. Notation is as follows: solid symbols, f_{lhr} = 300 Hz; open symbols, f_{lhr} = 1560 Hz; squares, lower estimate; circles, best estimate; stars, upper estimate.

Table 2. Auroral Hiss Source Locations

Hemisphere	Lower Cutoff	Upper Cutoff
Northern	$L = 5.587 \pm 0.001$	$L = 5.587 \pm 0.001$
	$Z_{cent} = 0.742 \pm 0.006$	$Z_{cent} = 0.617 \pm 0.007$
Southern	$L = 5.588 \pm 0.001$	$L = 5.589 \pm 0.001$
	$Z_{cent} = -0.550 \pm 0.007$	$Z_{cent} = -0.422 \pm 0.007$

Table 2 indicates a close agreement between L values for northward and southward sources. The values of Z_{cent}, the directed distance from the centrifugal equator, show a slight asymmetry of about 0.05 R_E. This is in all likelihood due to approximations involved in using (2) to determine the centrifugal equator. In spite of this small inaccuracy, the most symmetric pair of points is easily determined from Figure 10 or Table 2. If the 12 points of the 2 preferred source regions are used to get a mean and error on the mean, it is found that $L_{source} = 5.588 \pm 0.001$ and $|Z_{cent,source}| = 0.58 \pm 0.01\ R_J$. This result provides strong evidence that the sources of Jovian auroral hiss are at the north and south edges of the cold plasma torus and on the boundary between the hot and cold parts of the torus.

4. Interpretation

The location of the auroral hiss source at L slightly less than 5.6 invites comparison with known structures in the Io torus. Our result of $L_{source} = 5.588 \pm 0.001$ compares well with $L_{source} = 5.557 \pm 0.017$ cited by *Bagenal* [1989] as the crossover point between the hot and cold torus. She identifies this L shell as the boundary between inward and outward diffusing plasma and as the point of maximum flux tube content (density $\times L^2$ integrated along the flux tube).

Because the cold torus plasma diffuses "uphill" against the Jovian centrifugal potential, it diffuses slowly, allowing it to cool by radiation [*Barbosa and Moreno*, 1988]. This theory accounts for the cold torus but not for the well-defined density minimum observed between the two components of the torus.

In a seeming paradox the flux tube content maximum in the Io plasma torus nearly coincides with a minimum in the ion density along the spacecraft trajectory between 5.5 and 5.6 R_J. This coincidence can be clearly seen by comparing *Bagenal*'s [1985] Figure 7, showing flux tube content as a function of L value, and *Bagenal and Sullivan*'s [1981] Figure 6, showing charge density along the spacecraft trajectory as a function of L value. The flux tube content is an estimated integral of $L^2 \times$ the charge density over the length of the flux tube using a scale height approximation. Since the maximum in flux tube content is accompanied by a dip in temperature, it is apparent that the increase in scale height is due to an abrupt change in composition.

Trauger [1984] shows that densities of sulfur ions and electrons increase sharply around $L = 5.6$ and go through a maximum between $L = 5.6$ and $L = 5.9$. This high-density feature noted by Trauger is called the ribbon. Our results, taken in conjunction with those of *Bagenal* [1989] and *Trauger* [1984], indicate that the source of auroral hiss coincides with the torus maximum in flux tube content, the inward-outward diffusion boundary, and the inner edge of the ribbon.

As was pointed out in section 1, auroral hiss at Earth is known to be generated by electron beams traveling along magnetic field lines, and it is reasonable to assume that the same process occurs in the Io plasma torus. The result shown in Figure 10 leads us to conclude that field-aligned electron beams exist in the torus density minimum at a distance from the centrifugal symmetry surface corresponding to the northward and southward extent of the cold torus. Since auroral hiss is known to propagate in the same direction as the generating electron beam [*Gurnett et al.*, 1986], we conclude that there are two electron beams, generated at about 0.58 R_J north and south of the centrifugal symmetry surface in the torus density minimum, directed toward the centrifugal symmetry surface.

Magnetic-field-aligned electron beams are familiar objects in the Earth's auroral zone. The cause of these beams is generally believed to be an electric field component parallel to the magnetic field. Such electric fields are observed in connection with auroral displays [*Mozer and Fahleson*, 1970]. Oppositely directed, spikelike electric fields measured perpendicular to the magnetic field have been found to coincide with the edges of an inverted V event [*Gurnett*, 1972]. These spikes are what one would expect to see when the spacecraft flies through the edge of a localized region of parallel electric field, such as is thought to cause inverted V events (see Figures 9 and 10 of *Gurnett* [1972]). Thus electric fields are closely associated with the precipitating electrons that cause both the visual auroral displays and the downward propagating auroral hiss. *Block and Fälthammar* [1976] discuss five methods of creating an electric field in the magnetosphere. The favored method for creating electron beams is an electrostatic double layer, an electric field structure created by a spatial separation of electrons and ions along or oblique to a magnetic field line. The electric field created by this charge separation accelerates electrons in one direction and ions in the other, which creates both the electron beam that drives the auroral hiss and an ion beam in the opposite direction. In turn, the electrostatic double layer is known to be driven by a current [*Block*, 1975].

These relationships can be summarized as follows. The generation of auroral hiss depends on the existence of an electron beam. The most efficient way to create such a beam appears to be particle acceleration by a double layer. The double layer is in turn driven by a current. Thus the existence of auroral hiss implies the existence of a current. Since the auroral hiss radiates toward the centrifugal equator from the outer edges of the plasma torus, we deduce the existence of electron beams directed inward, toward the centrifugal equator. Since ions are accelerated by the double layer in the opposite direction, an ion beam should also exist, directed outward, away from the centrifugal equator. Thus our results imply a current directed along field lines northward and southward from the north and south edges of the hot-cold torus boundary, respectively. This situation is summed up schematically in Figure 11, taken from *Gurnett and Scarf* [1983]. It has been suggested that ion acceleration by this mechanism could be responsible for the existence of the torus density minimum (C. K. Goertz, personal communication, 1990). It should be noted that a preliminary examination of magnetometer data has not found evidence for field-aligned currents (M. Acuña, personal communication, 1994).

The electron beam associated with auroral hiss is part of the Jovian ionosphere-magnetosphere current system.

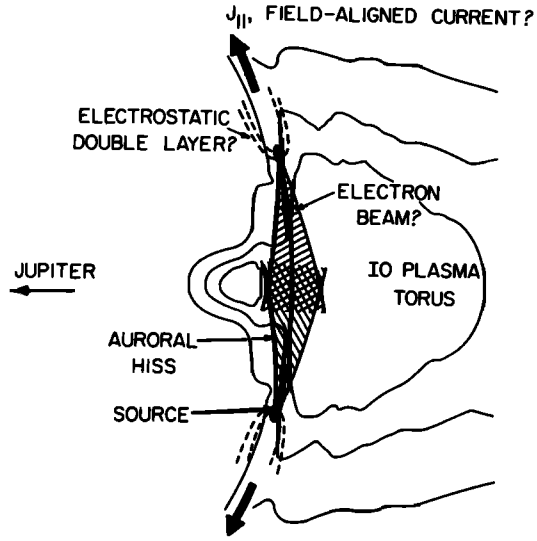

Figure 11. Schematic diagram showing the generation of the auroral hiss by electrostatic double layers on the hot-cold torus boundary at some distance north and south of the symmetry plane of the torus. (From *Gurnett and Scarf* [1983]. © Cambridge University Press 1983. Reprinted with the permission of Cambridge University Press.)

Therefore it is useful to review the physics of the interaction between the Jovian ionosphere and the Io plasma torus.

Magnetic field lines in the Jovian magnetosphere are highly conductive and essentially equipotential. Therefore the voltage drop generated by the ionosphere spinning in the presence of the Jovian magnetic field is carried on field lines out to the latitude of the plasma torus. This voltage drop causes an electric field that points radially outward through the torus. It is this electric field in conjunction with the Jovian magnetic field that causes the torus to corotate with the planet, and it is into this environment that Io releases large quantities of neutral sulfur and other materials. Material is ionized at a rate of about 10^3 kg/s [*Hill et al.*, 1983], and these new ions form a "pickup current" $\mathbf{J}_{pu}$ caused by ions and electrons gyrating in opposite directions at the time of ionization in the presence of an electric field. The expression given for this current by *Goertz* [1980] is $\mathbf{J}_{pu} = m_i S_i \mathbf{E}/B^2$, where S_i is the ion source strength and m_i is ion mass. The quantity $m_i S_i/B^2$ is called the pickup conductivity. The pickup conductivity is found to dominate the Pedersen conductivity by several orders of magnitude [*Hill et al.*, 1983]. For a further discussion of the pickup process, see *Belcher* [1987].

The pickup current is driven by the electric field generated in the ionosphere. This current is transmitted along magnetic field lines to the ionosphere, where it closes across magnetic field lines. This current system is shown schematically in Figure 12, adapted from *Belcher* [1987]. If we assume that the torus plasma is in a steady state, then the current density has a divergence of zero. In other words, all currents are closed and there is no net buildup of charge. Let us break the current density into $\mathbf{J}_\perp$ and $\mathbf{J}_{||}$ and let $\mathbf{J}_\perp$ be the pickup current density $\mathbf{J}_{pu}$. Then where $r^2\mathbf{J}_{pu}$ is constant, $\mathbf{J}_{||}$ must be 0; where $r^2\mathbf{J}_{pu}$ is increasing outward, $\mathbf{J}_{||}$ must be directed toward the plane of the torus; and where $r^2\mathbf{J}_{pu}$ is decreasing outward, $\mathbf{J}_{||}$ must be directed away from the plane of the torus. Therefore the most direct means of creating the current that drives the auroral hiss is for the pickup current to go through an abrupt outward decrease around $L = 5.6$. Such a variation could be occasioned by changes in either the radial electric field or in the pickup conductivity. Regarding electric field changes, *Bagenal* [1989] suggests that in parts of the torus, ionization could be strong enough that resulting charge buildup could shield parts of the torus from the electric field. This mechanism is more likely to occur near the orbit of Io, where ion densities are at least six orders of magnitude higher than they are near the torus density minimum. Another way to cause variation in radial electric field is by abruptly varying the potential transmitted along magnetic field lines from the Jovian ionosphere. In this case the L shell of the hot-cold torus boundary would be determined by varying conductivity in the ionosphere. It would seem to be something of a coincidence that the boundary would turn out to be so close to Io's orbit, although this is not impossible. A better possibility is variation in the pickup conductivity. Since the ion source strength depends on the densities of the various neutral atoms and the pickup conductivity depends on the ion mass, a change in pickup conductivity could be occasioned by an abrupt change in composition or in overall neutral density, a phenomenon that should be expected in the vicinity of Io. Ion source strengths are estimated only for O^+ and S^+ near the orbit of Io [*Hill et al.*, 1983]. Therefore an evaluation of the various possibilities is not currently possible.

Das and Ip [1992] have put forward the possibility that the beam of electrons is created by kinetic Alfvén waves generated in the region where the plasma density experiences its greatest parallel gradient. This mechanism could account for both the generation of a hiss-driving beam and energy input into the ribbon feature observed just outside the torus density minimum. Unfortunately, the beam generated by this mechanism is opposite in direction to the beam required to generate the auroral hiss observed around the Io plasma torus.

We have shown that the sources of auroral hiss in the Io plasma torus are electron beams nearly coincident with the inner edge of the plasma ribbon and the boundary between

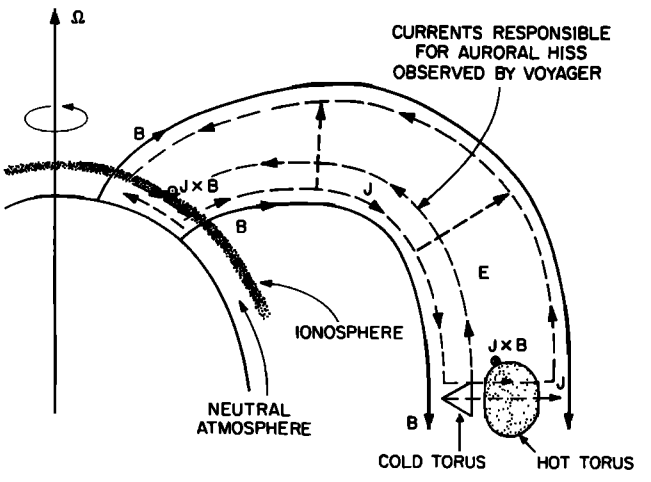

Figure 12. Schematic representation of Jovian ionosphere–Io torus interaction via Birkeland currents. The current driving the auroral hiss is shown between the hot and cold parts of the torus. (Adapted from *Belcher* [1987].)

inward and outward diffusion in the torus. These electron beams are probably associated with currents produced by electrostatic double layers at 0.58 R_J from the plane of the Io plasma torus. These double layers are very likely to be associated with changes in neutral density or composition brought about by differing conditions in the hot and cold parts of the plasma torus.

In section 2 we have noted a number of differences between the characteristics of the inbound and outbound events. We have also suggested that these differences are related to proximity to the satellite Io. There are two ways of interpreting these results. (1) The cause of the auroral hiss is directly related to the proximity of Io. According to this idea, the hiss should be most intense near Io, where it is being produced. The auroral hiss detected downstream of Io could be viewed as a "remnant" of the passing of Io, perhaps having to do with the Io plasma sheath or the motional potential across Io. Another explanation would have to do with the neutral cloud around Io, which is constantly in the process of being ionized. Since this cloud reaches well inside the orbit of Io, it could very well have a direct effect on the electric field structure and therefore on the current that drives the auroral hiss. This hypothesis is suggested by the outbound event being more intense than the inbound event near $L = 5.6$. In evaluating this hypothesis it should be recalled that the outbound event is only marginally more intense than the inbound event and then only near $L = 5.6$. (2) The auroral hiss is generated at all azimuths in the Io torus and is merely disturbed by the proximity of Io in the outbound event. That some aspect of Io disturbs the auroral hiss is suggested by the chaotic spectral appearance of the emission. The large range of L values over which the outbound event is visible, compared with the inbound event, implies either a more extended source or a larger angular range of emission. Candidates for the disturber of the plasma might be the Io neutral cloud or an Io bow wave. Of course, the auroral hiss could be both produced and disturbed due to proximity to Io. In future studies it will be interesting to see how the intensity of auroral hiss varies as a function of distance upstream and downstream from Io in order to establish whether the generating mechanism is associated with Io.

An indirect method of studying the effect of Io on the immediate environment is to use the coincidence we have noted between the current inferred from the auroral hiss and the plasma ribbon detected from the ground by *Trauger* [1984]. Ground-based observations of the ribbon, similar to those by *Trauger* [1984], could give us the location of the Birkeland current associated with auroral hiss as a function of azimuth. Such ground-based observations should be useful in determining whether the position and strength of this Birkeland current is a function of the position of Io. Thus if the field-aligned current that drives the auroral hiss is a response to the injection of material from Io, this should be evident from temporal variations in the position of the plasma ribbon, observable from the ground. In general, synoptic studies incorporating both ground-based and spacecraft observations should be a source of valuable insight in the future.

Acknowledgments. We acknowledge with pleasure a number of helpful discussions concerning the topic of this paper with the late Chris Goertz. This work was funded through contract 959193 with the Jet Propulsion Laboratory.

The Editor thanks J. L. Burch and another referee for their assistance in evaluating this paper.

References

Acuña, M. H., K. W. Behannon, and J. E. P. Connerney, Jupiter's magnetic field and magnetosphere, in *Physics of the Jovian Magnetosphere*, edited by A. J. Dessler, pp. 1–50, Cambridge University Press, New York, 1983.

Bagenal, F., Plasma conditions inside Io's orbit: Voyager measurements, *J. Geophys. Res.*, *90*(A1), 311–324, 1985.

Bagenal, F., Torus-magnetosphere coupling, in *Time-Variable Phenomena in the Jovian System*, edited by M. J. S. Belton, R. A. West, and J. Rahe, pp. 196–210, NASA, Washington, D. C., 1989.

Bagenal, F., and J. D. Sullivan, Direct plasma measurements in the Io torus and inner magnetosphere of Jupiter, *J. Geophys. Res.*, *86*(A10), 8447–8466, 1981.

Bagenal, F., R. L. McNutt Jr., J. W. Belcher, H. S. Bridge, and J. D. Sullivan, Revised ion temperature for Voyager plasma measurements in the Io plasma torus, *J. Geophys. Res.*, *90*(A2), 1755–1757, 1985.

Barbosa, D. D., and M. A. Moreno, A comprehensive model of ion diffusion and charge exchange in the cold Io torus, *J. Geophys. Res.*, *93*(A2), 823–836, 1988.

Belcher, J. W., The Jupiter-Io connection: An Alfvén engine in space, *Science*, *238*, 170–175, 1987.

Bell, T. F., and H. D. Ngo, Electrostatic lower hybrid waves excited by electromagnetic whistler mode waves scattering from planar magnetic field-aligned plasma density irregularities, *J. Geophys. Res.*, *95*(A1), 149–172, 1990.

Block, L. P., Double layers, in *Physics of the Hot Plasma in the Magnetosphere, Proceedings of the 30th Nobel Symposium, April 2–4, Kiruna, Sweden*, edited by B. Hultqvist and L. Stenflo, pp. 229–249, Plenum, New York, 1975.

Block, L. P., and C.-G. Fälthammar, Mechanisms that may support magnetic-field-aligned electric fields in the magnetosphere, *Ann. Geophys.*, *32*, 161–174, 1976.

Das, A. L., and W.-H. Ip, Particle-acceleration by kinetic Alfvén waves in the Io plasma torus, *Planet. Space Sci.*, *40*, 1499–1502, 1992.

Farrell, W. M., D. A. Gurnett, P. M. Banks, R. I. Bush, and W. J. Raitt, An analysis of whistler mode radiation from the Spacelab 2 electron beam, *J. Geophys. Res.*, *93*(A1), 153–161, 1988.

Farrell, W. M., D. A. Gurnett, and C. K. Goertz, Coherent Cerenkov radiation from the Spacelab 2 electron beam, *J. Geophys. Res.*, *94*, 443–452, 1989.

Farrell, W. M., R. J. MacDowall, M. D. Desch, M. L. Kaiser, R. G. Stone, N. Lin, N. Cornilleau-Wehrlin, P. Canu, S. J. Bame, and J. L. Phillips, Ulysses observations of auroral hiss at high Jovian latitudes, *Geophys. Res. Lett.*, *20*(20), 2259–2262, 1993.

Goertz, C. K., Io's interaction with the plasma torus, *J. Geophys. Res.*, *85*(A6), 2949–2956, 1980.

Gurnett, D. A., A satellite study of VLF hiss, *J. Geophys. Res.*, *71*(23), 5599–5615, 1966.

Gurnett, D. A., Electric field and plasma observations in the magnetosphere, paper presented at 1972 COSPAR Symposium on Critical Problems of Magnetospheric Physics, Comm. on Space Programs and Res., Int. Assoc. of Geomagn. and Aeron., Union Radio Sci. Int., Madrid, May 11–13, 1972.

Gurnett, D. A., and L. A. Frank, VLF hiss and related plasma observations in the polar magnetosphere, *J. Geophys. Res.*, *77*(1), 172–190, 1972.

Gurnett, D. A., and F. L. Scarf, Plasma waves in the Jovian magnetosphere, in *Physics of the Jovian Magnetosphere*, edited by A. J. Dessler, pp. 285–316, Cambridge University Press, New York, 1983.

Gurnett, D. A., W. S. Kurth, and F. L. Scarf, Auroral hiss observed near the Io plasma torus, *Nature*, *280*(5725), 767–770, 1979.

Gurnett, D. A., S. D. Shawhan, and R. R. Shaw, Auroral hiss, *Z* mode radiation, and auroral kilometric radiation in the polar magnetosphere: DE 1 observations, *J. Geophys. Res.*, *88*(A1), 329–340, 1983.

Gurnett, D. A., W. S. Kurth, J. T. Steinberg, P. M. Banks, R. I. Bush, and W. J. Raitt, Whistler-mode radiation from the Spacelab 2 electron beam, *Geophys. Res. Lett.*, *13*(3), 225–228, 1986.

Hill, T. W., A. J. Dessler, and F. C. Michel, Configuration of the Jovian magnetosphere, *Geophys. Res. Lett.*, *1*(1), 3–6, 1974.

Hill, T. W., A. J. Dessler, and C. K. Goertz, Magnetospheric Models, in *Physics of the Jovian Magnetosphere*, edited by A. J. Dessler, pp. 353–394, Cambridge University Press, New York, 1983.

James, H. G., VLF saucers, *J. Geophys. Res.*, *81*(4), 501–514, 1976.

Laaspere, T., and R. A. Hoffman, New results on the correlation between low-energy electrons and auroral hiss, *J. Geophys. Res.*, *81*(4), 524–530, 1976.

Lin, C. S., J. L. Burch, S. D. Shawhan, and D. A. Gurnett, Correlation of auroral hiss and upward electron beams near the polar cusp, *J. Geophys. Res.*, *89*(A2), 925–935, 1984.

Morgan, D. D., D. A. Gurnett, J. D. Menietti, J. D. Winningham, and J. L. Burch, Landau damping of auroral hiss, *J. Geophys. Res.*, *99*(A2), 2471–2488, 1994.

Mosier, S. R., and D. A. Gurnett, VLF measurements of the Poynting flux along the geomagnetic field with the Injun 5 satellite, *J. Geophys. Res.*, *74*(24), 5675–5687, 1969.

Mozer, F. S., and U. V. Fahleson, Parallel and perpendicular electric fields in an aurora, *Planet. Space Sci.*, *18*, 1563–1571, 1970.

Smith, R. L., VLF observations of auroral beams as sources of a class of emission, *Nature*, *224*(5217), 351–353, 1969.

Stix, T. H., *The Theory of Plasma Waves*, McGraw-Hill, New York, 1962.

Trauger, J. T., The Jovian nebula: A post-Voyager perspective, *Science*, *226*, 337–341, 1984.

F. Bagenal, Department of Astrophysical, Planetary, and Atmospheric Sciences, University of Colorado, Campus Box 391, Boulder, CO 80309-0391. (e-mail: bagenal@hao.ucar.edu)

D. A. Gurnett, W. S. Kurth, and D. D. Morgan, University of Iowa, Department of Physics and Astronomy, 203 Van Allen Hall, Iowa City, IA 52242-1479. (email: gurnett@iowave.physics.uiowa.edu; wsk@space.physics.uiowa.edu; ddm@space.physics.uiowa.edu)

(Received March 15, 1994; revised June 29, 1994; accepted July 18, 1994.)